

Effective utilization of coal fly ash containing unburned carbon

M. Miyake, V. Kumar Jha, Y. Kimura & M. Matsuda

*Department of Material and Energy Science,
Graduate School of Environmental Science, Okayama University,
Tsushima-Naka, Okayama 700-8530, Japan*

Abstract

We investigated the conversion process of coal fly ash with unburned carbon at greater than ca. 6 mass%, which has fallen behind in terms of resource recovery. As a result, composite materials consisting of zeolite A and/or zeolite X with good crystallinity and activated carbon were successfully prepared by NaOH fusion treatment at 750°C in N₂ flow followed by hydrothermal treatment. The type of zeolite phase formed was dependent on the hydrothermal treatment conditions including NaOH concentration. The resulting composite materials exhibited removal characteristics for heavy metal ions such as Ni²⁺, Cd²⁺ and Pb²⁺. In this paper, we describe the conversion of the main SiO₂-Al₂O₃ components and unburned carbon in coal fly ash into zeolite-activated carbon composite materials by a chemical process and the removal characteristics of the resulting materials.

Keywords: coal fly ash, zeolite, fusion treatment, hydrothermal treatment, removal characteristics.

1 Introduction

Fossil fuels are of great importance because they can be burned, producing significant amounts of energy. The burning of fossil fuels produces several billion tones of carbon dioxide per year globally. Therefore, in order to reduce the air pollution, several countries have put forward their environmental regulations. Under the regulations, coal-fired power plants will need to reduce their emissions by more than 50% within the next decade. Due to the strict regulations on the burning of coal, coal fly ash (CFA) contains variable amounts



of unburned carbon at less than *ca.* 20 mass%, depending upon the variations in the characteristics of different coal sources and coal-fired boilers. As the presence of such unburned carbon in CFA makes it difficult to use as a raw material for cement manufacturing and construction materials, much of CFA is ultimately dumped in landfills [1].

The reutilization of thus-dumped solid-waste CFA is the need of present context. Besides the utilization of bulk CFA, several potential uses of CFA have been reported as additives for the capture of industrial and water treatment wastes, sources of valuable metals, adsorbents for flue gas desulfurization, fireproofing materials, filter materials for the production of various products, ceramic applications and synthesis of several types of zeolites [2-14].

Owing to rich in Al_2O_3 and SiO_2 contents of CFA, the synthesis of zeolites by hydrothermal alkaline treatment is a promising technique for its reutilization. In addition to conventional hydrothermal alkaline treatment, there are a number of synthetic approaches to hydrothermal synthesis, such as a two-step method (fusion followed by hydrothermal treatment) [14-16] and the dry or molten-salt method [17]. These alternative methods were developed in order to achieve high synthesis efficiency and/or zeolite content. Furthermore, the presence of unburned carbon in CFA, which is burden for the utilization of bulk CFA, was successfully utilized by the two-step method [14]. Namely, the unburned carbon was converted into activated carbon, and composite materials consisting of zeolite X (Na-X) and/or zeolite A (Na-A) and activated carbon were prepared.

In the present study we have investigated the conversion process of unburned-carbon-contained-CFA into the composite of activated carbon and zeolites. The heavy metal ions removal characteristics of thus obtained composite materials were examined.

2 Materials and methods

2.1 Sample preparation and characterization

CFA used in this study was obtained from the Chugoku Electric Power Company Limited at Mizushima, Okayama, Japan. The chemical compositions of CFA were analyzed using X-ray fluorescence (XRF; Rigaku ZSX-100s). The average mass% of unburned carbon was analyzed by thermogravimetry-differential thermal analysis (TG-DTA; Rigaku TAS-100). The phases present in CFA was analyzed by powder X-ray diffractometer with monochromated $\text{CuK}\alpha$ radiation (XRD; Rigaku RINT2100/PC), and its shape and texture were observed using scanning electron microscope (SEM; JEOL JSM-6360FS).

CFA was mixed with NaOH with varying CFA/NaOH mass ratio 1-3 and fired at 750°C for 1 h in a N_2 atmosphere. After the NaOH fusion treatment, the mixture was ground and suspended in various amounts of deionized water (12-48 ml) in order to control NaOH concentration followed by stirring and aging for 2-24 h at room temperature. The slurry was sealed in a Teflon-lined autoclave and heated at 60-80°C for 2-24 h. After hydrothermal treatment, the sample was washed several times using deionized water, dried at 50°C overnight, and then collected for characterization.



The resulting materials were identified by XRD, and their specific surface areas were evaluated by measuring isothermal adsorption of N_2 at 77 K based on the BET method (BEL-Japan BELSORP 18 PLUS). The morphologies of the products were observed by SEM.

2.2 Uptake of metal ions

All the metal ion solutions were prepared separately, containing ppm concentrations of analytical grade metal chlorides, which were converted to mmol/L for later calculations. The resulting composite materials were subjected to Ni^{2+} , Cd^{2+} and Pb^{2+} removal experiments under the following conditions: temperature 25°C (room temperature), solid/solution ratio 100 mg/50 ml, initial metal ion concentrations 0.34–7.84 mmol/L of Ni^{2+} , 0.65–5.43 mmol/L of Cd^{2+} and 0.43–9.56 mmol/L of Pb^{2+} and treatment time 24 h. The kinetic experiments were also performed with same sample at constant metal ion concentrations (for Ni^{2+} , Cd^{2+} and Pb^{2+} at 4.46, 5.52 and 9.56 mmol/L, respectively) for times of 0.5–6 h.

After the removal experiments, the solid samples were filtered, washed several times with deionized water, dried at 50°C overnight, and identified by XRD. An atomic absorption spectrophotometer (Shimadzu AA-6800) was used to determine the concentrations of metal ions in the solutions before and after the removal experiments.

3 Results and discussion

3.1 Characterization of starting material and its products

The chemical compositions obtained by XRF and TG-DTA show that the major components of the CFA are SiO_2 , Al_2O_3 and unburned carbon (Table 1). The XRD traces (Fig. 1(a)) show that the major crystalline phases are α -quartz (SiO_2) and mullite ($3Al_2O_3 \cdot 2SiO_2$), together with amorphous components. The presence of spherical particles composed of aluminosilicate and big lumps of unburned carbon can be seen in the SEM micrograph (Fig. 1(b)). The specific surface area of as-received CFA was found to have *ca.* 6 m²/g.

Table 1: Chemical composition of coal fly ash (CFA).

Component	SiO_2	Al_2O_3	CaO	C	Fe_2O_3	TiO_2	MgO	K_2O	Other
mass%	50.9	26.2	4.5	8.0	4.3	1.5	1.3	1.1	2.2

In order to determine the optimum conversion conditions and to obtain Na-X or Na-A with good crystallinity, several parameters such as NaOH/CFA ratio, aging time, NaOH concentration by adding various amount of water, reaction time and temperature were varied. The fusion temperature was based on the activation temperature in the general preparation of activated carbon [18].



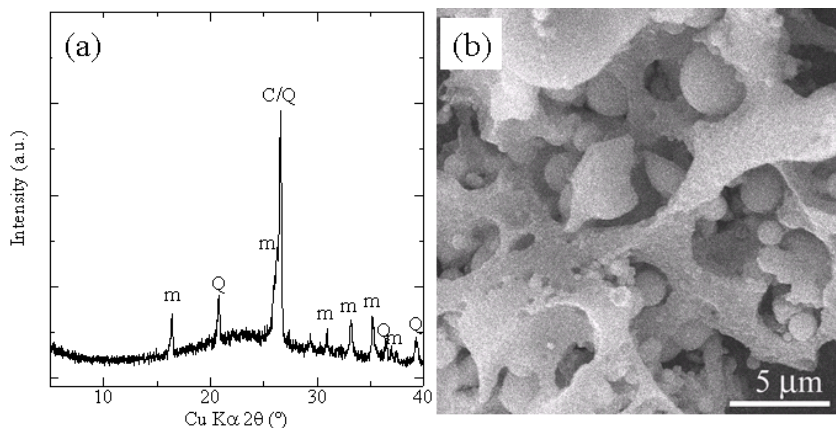


Figure 1: (a) XRD pattern and (b) SEM micrograph of as-received CFA. Symbols: C- unburned carbon, Q- quartz and m- mullite.

The specific surface area and the pore size distribution, evaluated by N_2 adsorption isotherm measurement of treated CFA as a function of NaOH/CFA ratio, suggested maximum surface area and formation of mesopores at the optimum mass ratio of 2. In order to find the influence of the aging time, the fused CFA was subjected to the variation of aging time in between 2-24 h before the hydrothermal treatment. The crystallinity of Na-X was strengthened while that of Na-A was weakened with elongation of aging time. Furthermore the crystallinities of both Na-X and Na-A were strengthened at 2 h aging times with the variation of the amount of water. Thus, NaOH/CFA mass ratio of 2 and the aging time of 2 h were decided as the optimum conditions before the variations of amounts of water, reaction time and temperature for hydrothermal treatments of treated CFA.

In order to determine the effect of NaOH concentration on the product, the fused CFA was suspended in various amounts of water (12-48 ml) followed by aging for 2 h, and the suspension was hydrothermally treated at 80°C for 24 h. The XRD patterns of the resulting materials with the variation of amounts of water are shown in Fig. 2. At 12 ml water, Na-X with good crystallinity was formed. The peak intensities of Na-X were weakened with increasing amount of water, while the peaks of Na-A were strengthened. At 30 ml water, almost single phase Na-A was obtained, whereas with further increasing amount of water to 48 ml, the sample became completely amorphous suggesting the formation of geopolymer. The Si/Al molar ratio of Na-A is 1 while that in CFA is ca. 2. This indicates the presence of amorphous SiO_2 along with Na-A.

Next, reaction temperature (60-120°C) and time (2-24 h) were examined. Consequently, the crystallinities of Na-X and Na-A obtained by hydrothermal treatments for 24 h were promoted with increasing reaction temperature up to 80°C. They were, however, decomposed and transformed into sodalite above 100°C. Na-X and Na-A with good crystallinities were produced at 80°C within 24 h. Thus, the reaction temperature and time were set at 80°C and 24 h, respectively.

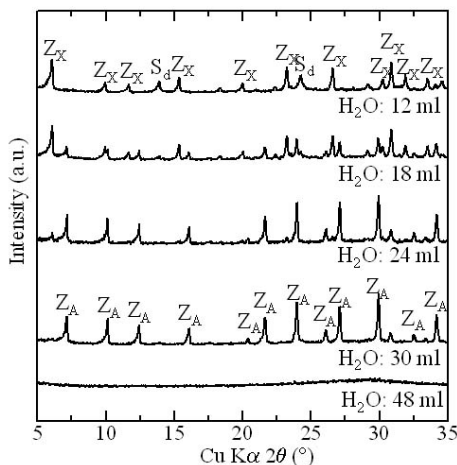


Figure 2: XRD patterns of products from CFA with variation of amounts of water. Symbol: Z_A - Na-A, Z_X - Na-X and S_d - sodalite.

3.2 Metal ion sorption isotherms

The larger size of window cage and higher concentration of Na^+ of Na-X are favorable features for its higher metal ion sorption capacity. Hence the removal characteristics of Ni^{2+} , Cd^{2+} and Pb^{2+} were carried out with Na-X material obtained from CFA. The plots of the release of Na^+ as a function of metal ion sorption show that the removal reactions for these metals progress principally by cation exchange, because the molar ratio of $\text{M}^{2+}/\text{Na}^+$ is approximately 2.

The sorption isotherms of Me^{2+} ($\text{Me} = \text{Ni}, \text{Cd}$ and Pb) were simulated by mathematical equations of Langmuir [19] and Freundlich and Heller [20]. The Langmuir model assumes that the removal of metal ion occurs on a homogenous surface by monolayer sorption, and predicts a linear relation between (C_e/Q_e) and C_e .

$$\left(\frac{C_e}{Q_e}\right) = \left(\frac{1}{Q_{\max}}\right)C_e + \left(\frac{1}{Q_{\max} \cdot b}\right) \quad (1)$$

where C_e (mmol/L) is the equilibrium concentration, Q_e (mmol/g) is the amount sorbed at equilibrium, Q_{\max} (mmol/g) is the monolayer sorption capacity and b (L/mmol) is the Langmuir constant.

On the other hand, the Freundlich model, which is encompassing the surface heterogeneity and exponential distribution of active sites, provides an empirical relationship between the sorption capacity and equilibrium constant of the sorbent. The mathematical representation of this model in linear form is

$$\text{Log}Q_e = \frac{1}{n}\text{Log}C_e + \text{Log}K_f \quad (2)$$

where, K_f (mmol/g) and n (g/L) are the Freundlich constants related to the sorption capacity and sorption affinity of the sorbent, respectively.

The resulting sorption isotherms are shown in Fig. 3. The parameters calculated from the Langmuir and Freundlich equations using the experimental data are listed in Table 2. The solid and dash line curves in Fig. 3 are calculated from the resulting Langmuir and Freundlich parameters, respectively. The statistical analyses (Table 2) indicated that the Langmuir isotherm could characterize the sorption with a high correlation coefficient values suggesting that the sorption isotherms are of the Langmuir type. The resulting Q_{\max} values decrease in the order $\text{Pb}^{2+} > \text{Cd}^{2+} > \text{Ni}^{2+}$.

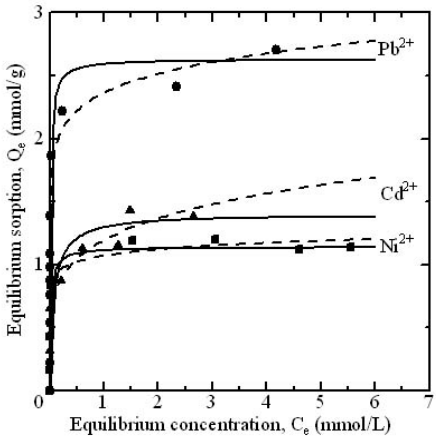


Figure 3: Sorption isotherms of Ni^{2+} , Cd^{2+} and Pb^{2+} by Na-X obtained from CFA. Solid and dash lines represent predicted data from Langmuir and Freundlich parameters, respectively.

Table 2: Parameters of isotherms for sorption of Ni^{2+} , Cd^{2+} and Pb^{2+} by Na-X obtained from CFA.

Me^{2+}	Langmuir's parameters			Freundlich's parameters		
	b	Q_{\max}	R^2	n	K_f	R^2
	(L/mmol)	(mmol/g)		(g/L)	(mmol/g)	
Ni^{2+}	44.5	1.14	0.9991	15.5	1.07	0.8524
Cd^{2+}	12.9	1.40	0.9881	5.2	1.20	0.8722
Pb^{2+}	67.9	2.63	0.9971	11.2	2.63	0.8844

This metal ion removal series is in agreement with those previously reported for Na-A [21], Na-P1 [22] and clinoptilolite [23]. The electronic configurations of Pb^{2+} and Cd^{2+} are d^{10} and hence have zero-ligand-field stabilization in octahedral aqua complexes. Thus Pb^{2+} and Cd^{2+} interact strongly with the zeolite framework during the metal ion removal process in comparison to Ni^{2+} , whose electronic configuration is d^8 [21].



3.3 Sorption kinetics

The sorption of metal ions (Ni^{2+} , Cd^{2+} and Pb^{2+}) by Na-X obtained from CFA as a function of contact time is shown in Fig. 4. These plots indicate that the sorption progresses in two steps, initially the rapid sorption within 30 minutes followed by a slower second step during which equilibrium is attained. This behavior of sorption is consistent with previously reported [24, 25]. The rapid step is due to the abundant availability of active sites on the sorbent material, and as these sites become increasingly occupied, the sorption becomes less efficient and slower.

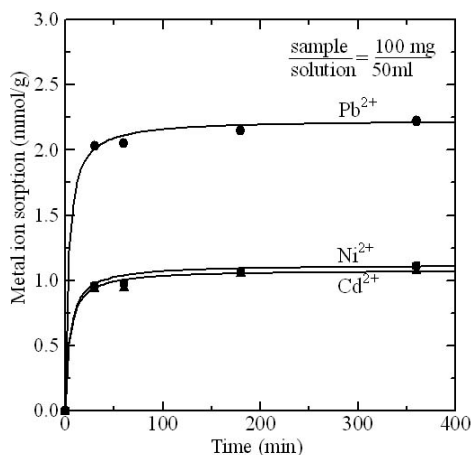


Figure 4: Plots of metal ions sorbed on Na-X prepared from CFA as a function of contact time. Solid lines represent predicted data by a pseudo-second order model.

In order to investigate the rate law describing the metal ion sorption, the kinetic data obtained from the batch experiments were analyzed using two kinetic equations, *namely*, the first-order equations proposed by Lagergren and Svenska [26] and the pseudo-second order equation proposed by Ho *et al.* [27]. The equations were rearranged to obtain the linear forms as follows:

$$\text{Log}(Q_e - Q_t) = \text{Log}Q_e - \frac{K_1}{2.303} t \quad (3)$$

$$\frac{t}{Q_t} = \frac{1}{(K_2 Q_e^2)} + \frac{1}{Q_e} t \quad (4)$$

where Q_t is the amount adsorbed (mmol/g) at time t (min), C_e and Q_e are as in equation (1), K_1 and K_2 are rate constants of equations (3) and (4), respectively. Equations (3) and (4) yielded the rate constants (K_1 and K_2) and the equilibrium metal ion sorption Q_e , presented in Table 3. The Q_e values obtained from the pseudo-second order equation (4) are comparable with the Q_{\max} values obtained from the Langmuir equation (1) (Table 2), indicating the pseudo-second order reaction model is more appropriate for metal ion sorption.



Table 3: Kinetic data for Na-X estimated from various equations.

System	K ₁ from equation (3)	K ₂ from equation (4)	Q _e (mmol/g) from	
			equation (3)	equation (4)
Ni ²⁺	4.6×10 ⁻³	0.20	1.97	1.12
Cd ²⁺	1.0×10 ⁻³	0.21	3.35	1.08
Pb ²⁺	1.2×10 ⁻³	0.14	1.23	2.23

4 Conclusion

Na-X and Na-A zeolites were successfully obtained from CFA. The appropriate conditions for Na-X were found to be as: NaOH fusion temperature 750°C, amount of water 12 ml, reaction temperature 80°C, longer aging time and reaction time 24 h while those for Na-A are similar to those of Na-X except the amount of water in between 24-30 ml and shorter aging time.

Thus obtained composite materials have good sorption characteristics for heavy metals, with sorption isotherm more favorable to Langmuir model. The equilibrium sorption capacity follows the order Pb²⁺ > Cd²⁺ > Ni²⁺. The high removal of Pb²⁺ and Cd²⁺ was expected to be due to the ligand-field stabilization. The overall sorption process was pseudo-second order with an initial rapid and quantitatively predominant sorption followed by a second slower and quantitatively insignificant sorption.

Acknowledgements

This work was supported by a Grant-in-Aid from Okayama Prefectural Government and Okayama Prefecture Industrial Promotion Foundation, and in part by a Grant-in-Aid from the Okayama University 21st Century COE program "Strategic Solid Waste Management for Sustainable Society".

References

- [1] Baltrus, J.P., Wells, A.W., Fauth, D.J., Diehl, J.R. and White, C.M., Characterization of Carbon Concentrates from Coal-Combustion Fly Ash, *Energy & Fuels*, **15**, pp. 455-462, 2001.
- [2] Jha, V.K., Matsuda, M., Miyake, M., Resource recovery from coal fly ash waste: an overview study, *Journal of the Ceramic Society of Japan*, **116**, 2008.
- [3] Dirk, G., Pulverised fuel ash products solve the sewage sludge problems of the wastewater industry, *Waste Management*, **16**, 51-57 (1996).
- [4] Andres, A., Ortiz, I., Viguri, J.R. and Irabien, A., Long-term behaviour of toxic metals in stabilized steel foundry dusts, *Journal of Hazardous Materials*, **40**, pp. 31-42, 1995.



- [5] Pickles, C.A., McLean, A., Alcock, C.B. and Nikolic, R.N., Plasma recovery of metal values from fly ash, *Canadian Metallurgical Quarterly*, **29**, pp. 193–200, 1990.
- [6] Font, O., Querol, X., Plana, F., López-Soler, A., Chimenos, J.M., March, M.J., Espiell, F., Burgos, S., García, F. and Alliman, C., Occurrence and distribution of valuable metals in fly ash from Puertollano IGCC power plant, Spain, *International Ash Utilization Symposium, 22–24 October, Hyatt Regency Lexington, Lexington, KY, USA*, 2001.
- [7] Garea, A., Viguri, J.R. and Irabien, A., Kinetics of flue gas desulphurization at low temperatures: fly ash/calcium (3/1) sorbent behavior, *Chemical Engineering Science*, **52**, pp. 715–732, 1997.
- [8] Vilches, L.F., Fernández-Pereira, C., Olivares, J., Rodríguez Piñeiro, M. and Vale, J., Development of new fire-proof products made from coal fly ash, *PROGRES Workshop on Novel Products from Combustion Residues, Morella, Spain*, pp. 343–351, 2001.
- [9] Kruger, R.A., Fly ash beneficiation in South Africa: creating new opportunities in the market-place, *Fuel*, **76**, pp. 777–779, 1997.
- [10] Anderson, M. and Jackson, G., The beneficiation of power station coal ash and its use in heavy clayware ceramics, *British Ceramic Transactions and Journal*, **82**, pp. 34–42, 1983.
- [11] Stoch, L., Kordek M. and Nadachowski, F., Processing of some non-conventional ceramic raw materials and by-products, *Ceramics International*, **12**, pp. 213–220, 1986.
- [12] Queralt, I., Querol, X., López-Soler, A. and Plana, F., Use of coal fly ash for ceramics: a case study for a large Spanish power station, *Fuel*, **76**, pp. 787–791, 1997.
- [13] Querol, X., Moreno, N., Umaña, J.C., Alastuey, A., Hernández, E., López-Soler, A. and Plana, F., Synthesis of zeolites from coal fly ash: an overview, *International Journal of Coal Geology*, **50**, pp. 413–423, 2002.
- [14] Miyake, M., Kimura, Y., Ohashi, T., and Matsuda, M., Preparation of activated carbon–zeolite composite materials from coal fly ash, *Microporous and Mesoporous Materials*, In press.
- [15] Shigemoto, N., Hayashi, H., and Miyaura, K., Selective formation of Na–X, zeolite from coal fly ash by fusion with sodium hydroxide prior to hydrothermal reaction, *Journal of Materials Science*, **28**, pp. 4781–4786, 1993.
- [16] Hollman, G.G., Steenbruggen, G. and Janssen-Jurkovičová, M., A two-step process for the synthesis of zeolites from coal fly ash, *Fuel*, **78**, pp. 1225–1230, 1999.
- [17] Park, M., Choi, C.L., Lim, W.M., Kim, M.C., Choi, J. and Heo, N.H., Molten-salt method for the synthesis of zeolitic materials. I. Zeolite formation in alkaline molten-salt system, *Microporous and Mesoporous Materials*, **37**, pp. 81–89, 2000.
- [18] Sanada, Y., Suzuki, M., and Fujimoto, K. (Eds), *Shinpan-Kasseitan* (in Japanese). Kodansha Scientific Co., Tokyo, pp.51-54, 1992.



- [19] Langmuir, I.J., The adsorption of gases on plane surfaces of glass, mica and platinum, *Journal of the American Chemical Society*, **40**, pp.1361-1403, 1918.
- [20] Freundlich, H. and Heller, W., The adsorption of cis- and trans-azobenzene, *Journal of the American Chemical Society*, **61**, pp. 2228-2230, 1939.
- [21] Majdan, M., Pikus, S., Kowalska-Ternes, M., Gładysz-Płaska, A., Staszczuk, P., Fuks, L. and Skrzypek, H., Equilibrium study of selected divalent d-electron metals adsorption on A-type zeolite, *Journal of Colloid and Interface Science*, **262**, pp. 321-330, 2003.
- [22] Steenbruggen, G. and Hollman, G.G., The synthesis of zeolites from fly ash and the properties of the zeolite products, *Journal of Geochemical Exploration*, **62**, pp. 305-309, 1998.
- [23] Ouki, S.K. and Kavanagh, M., Performance of natural zeolites for the treatment of mixed metal-contaminated effluents, *Waste Management and Research*, **15**, pp. 383-394, 1997.
- [24] Sag, Y. and Kutsal, T., The selective biosorption of chromium(VI) and copper(II) ions from binary metal mixtures by *R. arrhizus*, *Process Biochemistry*, **31**, pp. 561-572, 1996.
- [25] Nouri, L., Ghodbane, I., Hamdaoui, O. and Chiha, M., Batch sorption dynamics and equilibrium for the removal of cadmium ions from aqueous phase using wheat bran, *Journal of Hazardous Materials*, **149**, pp. 115-125, 2007.
- [26] Lagergren, S. and Svenska, B.R., Zur theorie der sogenannten adsorption geloester stoffe, *Veternskapsakad Handlinger*, **24**, pp. 1-39, 1898.
- [27] Ho, Y.S., Chiu, W.T., Hsu, C.S. and Huang, C.T., Sorption of lead ions from aqueous solution using tree fern as a sorbent, *Hydrometallurgy*, **73**, pp. 55-61, 2004.

